Intrazeolite Nanocomposite Catalysts: Co-Mo Sulfides for Hydrodesulfurization

Yasuaki Okamoto and Hiromoto Katsuyama
Dept. of Chemical Engineering, Osaka University, Osaka 560, Japan

It was, for the first time, demonstrated by means of FTIR, EXAFS, XPS, and XRF techniques that thermally stable Co – Mo binary sulfide clusters were synthesized in NaY zeolite cavities using Co and Mo carbonyls as precursors. The hydrodesulfurization (HDS) and hydrogenation activities of the intrazeolite nanocomposite sulfide clusters were examined as a function of composition. It was found that the highest HDS activity was attained at Co/Mo ≃ 1 (2 Mo/super cage or 12 wt. % Mo) and that the Co sites of the clusters were responsible for the reactions. The composition of the catalytically active intrazeolite Co – Mo sulfide clusters was implied to be $Co_2Mo_2S_6$. The present intrazeolite nanostructure approach strongly suggested that the Co – Mo binary sulfide formation played a prominent role in the catalytic synergy generation. Metal carbonyl techniques were used in the preparation of intrazeolite Fe – Mo binary sulfides.

Introduction

Zeolites possess unique properties as catalyst supports; well-defined and ordered pore structure on a molecular level, high thermal stability, and high surface area (Breck, 1974). The pore size, electronic states, and acid-base nature of zeolites can be controlled by crystal structure, composition, or an extra-framework cation (Breck, 1974; Mortier and Schoonheydt, 1985; Rabo and Gajda, 1989/1990; Okamoto, 1995b). When well-characterized precursors are used for preparation, uniform and well-defined nanostructures in ordered arrays are thereby anticipated to form in zeolite cavities. From the viewpoint of catalysis, the preparations of uniform and catalytically active clusters encaged in zeolite are thought to lead to highly selective catalysts modified by molecular sieving effects, and to facilitate an understanding of the relationship between the catalyst structure and catalysis. Intrinsically, high dispersions of the intrazeolite clusters may bring about highly active catalysts.

Encapsulation of metal complexes in zeolite cavities and the synthesis of metal clusters from appropriate precursor complexes have been extensively studied for the development of a novel type of catalysts, and some of them are employed in the chemical industry (Ichikawa, 1992; Sachtler and Zhang, 1993; Gates, 1995). Preparations of intrazeolite metal oxide or sulfide clusters with well-defined nuclearities and structures, however, have been examined much less: W (Ozin and Özkar, 1990; Moller et al., 1991; Ozin et al., 1992a,b), Mo (Ozin et al., 1992b; Okamoto et al., 1993), and Fe (Bein et al., 1986a,b; Okamoto et al., 1996b); oxides synthesized by oxidizing the corresponding metal carbonyls and Cd (Wang and Herron, 1987, 1988; Herron et al., 1989; Fox and Pettit, 1989; Liu and Thomas, 1989; Wark et al., 1991), Zn (Fox and Pettit, 1989), and Pb (Wang and Herron, 1987; Wark et al., 1991); sulfide clusters by sulfidation of cation-exchanged zeolites. Extended X-ray absorption fine structure (EXAFS) studies showed the formations of uniform nanoclusters with well-defined structures characteristic of the pore structure of the host zeolite. Some of these nanostructures exhibit quantum-sized effects for photoabsorptions (Stucky and MacDougall, 1990). However, the catalytic properties of the oxide or sulfide species thus prepared have scarcely been investigated. In our previous study, it was shown that intrazeolite iron oxide clusters prepared using $Fe(CO)_5$ exhibited high activities for the reduction of NO by CO and for the selective oxidation of 1-butene to butadiene (Okamoto et al., 1996b). Molybdenum sulfide clusters encaged in a zeolite were found to be prepared by sulfiding $Mo(CO)_6$ encaged in a NaY zeolite (Okamoto et al., 1988, 1989a; Laniecki and Zmierczak, 1991; Vorbeck et al., 1994; Okamoto and Katsuyama, 1996a; Okamoto et al. 1996c; Sakamoto et al., 1996), and to show significantly higher hydrodesulfurization and hydrogenation activities than those prepared by a conventional impregna-

Correspondence concerning this article should be addressed to Y. Okamoto.
Present addresses of Y. Okamato: Dept. of Materials Science, Shimane University, Matsue 690, Japan and Crest, Japan Science and Technology Corp., Japan.

tion method. Besides, quantum-sized metal sulfide or oxide particles are considered to be promising as photocatalysts, too.

Practical catalysts usually consist of several synergistic components; for instance, a main catalytic component and promoters (Gates et al., 1979). Extensive research has been conducted to reveal the origin of synergy generation between these ingredients. In order to understand the precise mechanism of catalytic synergy generation, and thus for the design of a novel type of composite catalyst, it is considered promising to fabricate zeolite-encaged composite clusters with a uniform composition and structure. To our knowledge, however, no intrazeolite nanocomposite oxide or sulfide clusters have been synthesized in well-characterized forms, despite the great importance of composite systems for catalysts. In the present study, we tried to prepare Co–Mo binary sulfide clusters encapsulated in a NaY zeolite.

Co–Mo binary sulfide systems are widely used as hydrotreating catalysts in the petroleum industry (Schuit and Gates, 1973; Gates et al., 1979; Topsøe and Clausen, 1984; Topsøe et al., 1986; Prins et al., 1989; Delmon, 1993; Chianelli et al., 1994; Topsøe et al., 1996). It is well established that strong catalytic synergies pass between Co and Mo sulfides, for example, for hydrodesulfurization reactions. The origin of the synergy generation in Co–Mo systems is still controversial (Prins et al., 1989; Delmon, 1993; Chianelli et al., 1994; Topsøe et al., 1996). The present intrazeolite nanocomposite approach strongly suggested that Co–Mo binary sulfide formation is important for the synergy generation.

Experimental Studies

Catalyst preparation

After evacuation at 673 K for 1 h (1×10^{-3} Pa), a NaY zeolite possessing a Si/Al atomic ratio of 2.1 (Shokubai Kasei Kogyo Ltd., Japan) was exposed to a vapor of $Mo(CO)_6$, $Co(CO)_3NO$, or $Fe(CO)_5$ at room temperature, followed by an evacuation at room temperature for 10 min to remove physisorbed metal carbonyl molecules on the external surface of the zeolite. The amount of the metal carbonyl adsorption in zeolite was controlled by the adsorption time, the repetition cycle of the adsorption, and the amount of a dose using a known volume of vapor. A saturated adsorption of $Mo(CO)_6$ took about 16 h, while a saturation was attained within a few minutes for $Co(CO)_3NO$ or $Fe(CO)_5$. $Mo(CO)_6$/NaY, $Co(CO)_3NO$/NaY, or $Fe(CO)_5$/NaY thus prepared was sulfided in a stream with an atmospheric pressure of 10% H_2S/H_2. The sulfidation temperature was increased from room temperature to 373 K at a rate of 2 K min^{-1} and held at 373 K for 1 h. Subsequently, the temperature was ramped to 673 K at a rate of 5 K min^{-1} and held at the temperature for 1.5 h. After the sulfidation, the sample was cooled in the H_2S/H_2 stream to room temperature. The metal sulfide catalysts thus prepared are denoted $MoSx$/NaY, $CoSx$/NaY, or $FeSx$/NaY. Mo sulfide catalysts, MoS_2/NaY, were also prepared by a conventional impregnation method using ammonium heptamolybdate, for comparison. The catalyst precursor was calcined in air at 773 K for 5 h.

Binary sulfide catalysts—$CoSx$–$MoSx$/NaY catalysts—were synthesized by introducing $Co(CO)_3NO$ into $MoSx$/NaY after an evacuation at 673 K for 1 h, followed by a second temperature-programmed sulfidation at 673 K for 1.5 h. $Co_2(CO)_8$ dispersed in *n*-heptane was also examined instead of $Co(CO)_3NO$ to prepare zeolite-supported Co–Mo binary sulfides. A known amount of a degassed $Co_2(CO)_8$/*n*-heptane solution was admitted to $MoSx$/NaY or MoS_2/NaY in vacuum through a breakable joint while shaking well. After removing the solvent by evacuation at room temperature, the sample was sulfided in the same manner as the $Co(CO)_3NO$-derived catalysts. The catalyst sample prepared using $Co_2(CO)_8$ is denoted here, for example, $CoSx$/$MoSx$/NaY.

The Co and Mo contents of the sulfide catalysts were determined by chemical analysis (AAS and ICP). For the sake of the elemental analysis of the sulfide catalyst, X-ray fluorescence (XRF, Rigaku Industrial Corp., RIX3001) measurements were conducted under a He stream to minimize degradation of the sample during the XRF analysis.

Reaction procedure

The hydrodesulfurization (HDS) of thiophene and hydrogenation (HYD) of butadiene were carried out over the sulfide catalysts (0.1 g) using a circulation system (0.20 dm^3) made of glass. The details of the procedures have been reported elsewhere (Okamoto et al., 1995a, 1996a). Briefly, the HDS of thiophene was carried out at 623 K and at an initial total pressure of 20 kPa ($H_2/C_4H_4S = 36$). The thiophene pressure was kept constant (0.54 kPa) during the reaction by holding a small amount of liquid thiophene kept at 273 K as a reservoir in the bottom of a U-tube in the circulation system. The activity was evaluated by the amount of H_2S evolved during the reaction. The HYD of butadiene was conducted at 473 K over the catalyst, which had been used for the HDS reaction for 1 h and subsequently evacuated at 673 K for 1 h. The initial pressure of the reaction gas was 14 kPa ($H_2/C_4H_6 = 2$). The reaction gas was analyzed by means of an on-line gas chromatography.

Catalyst characterization

The Mo and Co *K*-edge EXAFS spectra for the catalysts and reference compounds were measured on the BL-10B and 6B, respectively, at the Photon Factory of the National Laboratory for High Energy Physics by means of synchrotron radiation. The EXAFS spectra were obtained at room temperature using an *in situ* EXAFS cell with Kapton windows. Data analysis was conducted assuming a plane-wave approximation. Details of the procedures have been published elsewhere (Okamoto et al., 1991, 1995a).

The X-ray photoelectron spectroscopy (XPS) data of the catalysts were obtained on an XPS-7000 photoelectron spectrometer (Rigaku Industrial Corp., Al anode; 1486.6 eV). The sample was mounted on a sample holder in a glove bag filled with high-purity Ar. The binding energies were referenced to the Si2*p* level at 103.0 eV for the NaY zeolite, which had been determined by the C1*s* level at 285.0 eV due to adventitious carbon.

The FTIR spectra of NO adsorption on the catalyst were measured on a JEOL JIR-100 spectrophotometer in a diffuse reflectance mode. After a background spectrum was measured *in situ* for a freshly sulfided catalyst at 673 K, NO was introduced to the catalyst as an NO/He pulse (10% NO, 5.1

cm^3). The spectra were recorded after admission of five pulses. The IR spectra of the NO adsorption on MoSx/NaY were measured in the transmission mode using an *in situ* cell on a Hitachi double-beam spectrophotometer (EPI-G).

Results

Mo, Co, and Fe Sulfides Encaged in NaY

The number of $Mo(CO)_6$ molecules accommodated in each supercage (SC) was saturated at 1.9–2.1 Mo/SC or 12 wt. % Mo with respect to NaY, in agreement with the results by other workers (Komatsu et al., 1985; Yong and Howe, 1986). The HDS activities of MoSx/NaY and MoS_2/NaY are shown in Figure 1 as a function of the Mo content as expressed by Mo atoms/SC. The activity of MoSx/NaY linearly increased up to 2Mo/SC, followed by a leveling off of activity at a higher Mo content. MoSx/NaY catalysts were 3–4 times more active than MoS_2/NaY, in conformity with the results obtained using a fixed-bed flow reactor (Okamoto et al., 1988, 1989a). Although the catalytic activities obtained using the present circulation system are initial ones of the fresh catalysts, relative HDS activities of the catalysts in Figure 1 are considered to represent relative steady-state activities.

Figure 2 shows the catalytic activities of NaY-supported Mo sulfides for the HYD of butadiene as a function of Mo content. Mo-loading effects similar to those for HDS were observed, and the HYD(473 K)/HDS (623 K) activity ratio was 0.45–0.50, irrespective of the Mo-loading and-preparation methods.

The dispersion and structure of the Mo sulfide species in MoSx/NaY and MoS_2/NaY were examined using EXAFS techniques. The k^3-weighted Fourier transforms of Mo K-edge EXAFS are depicted in Figure 3. The structural parameters derived from EXAFS analysis are summarized in Table 1. Detailed analysis of EXAFS data of MoSx/NaY and MoS_2/NaY was reported elsewhere (Okamoto et al., 1996a). With MoSx/NaY, only Mo–S and Mo–Mo bondings were observed, indicating a complete sulfidation of $Mo(CO)_6$ to Mo sulfide species. A significantly low coordination number of Mo–Mo bondings (ca., unity) suggests that the Mo sulfide species in MoSx/NaY are highly dispersed, possibly forming

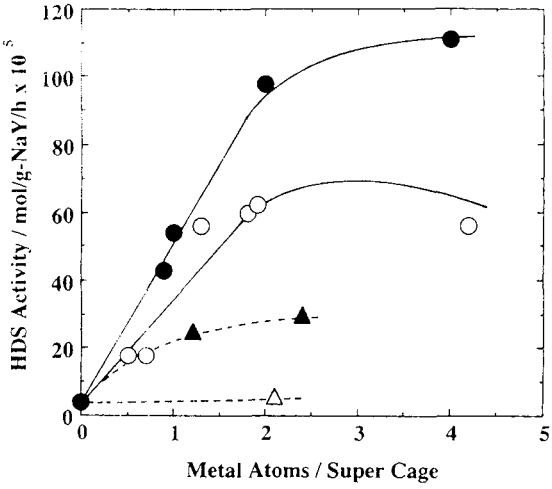

Figure 1. Activity of a NaY-supported metal sulfide catalyst for hydrodesulfurization of thiophene as a function of metal loading as expressed by metal atoms/SC.

●: MoSx/NaY; ▲: MoS_2/NaY; ○: CoSx/NaY; and △: FeSx/NaY.

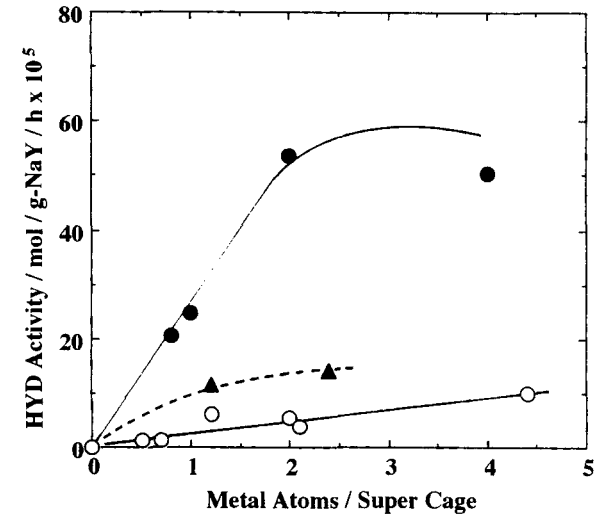

Figure 2. Activity of a NaY-supported metal sulfide catalyst for hydrogenation of butadiene as a function of metal loading as expressed by metal atoms/SC.

●: MoSx/NaY; ▲: MoS_2/NaY; and ○: CoSx/NaY.

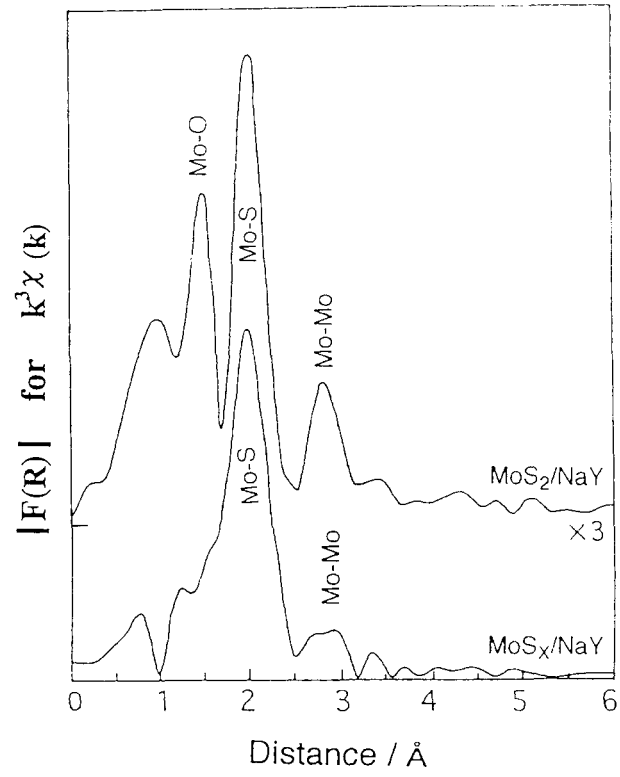

Figure 3. Fourier transforms of k^3-weighted EXAFS modulations (Δk = 4–15 $Å^{-1}$) of the Mo K-edge for MoSx/NaY (2 Mo/SC) and MoS_2/NaY (0.8 Mo/SC, sulfided for 5 h).

Table 1. Structural Parameters* as Derived from the Mo *K*-Edge EXAFS for Mo, Co-Mo, and Fe-Mo Sulfide Catalysts Encaged in a NaY Zeolite

Catalyst	Loadings/SC** Mo	Co/Fe	Bondings	*R*/Å	*CN*	E_0/eV	$\Delta\sigma^2$/Å^2
MoS*x*/NaY†	2.1	—	Mo–S	2.40	4.7	−2.3	0.0048
			Mo–Mo	3.15	1.1	−2.0	0.0089
MoS_2/NaY††	0.8	—	Mo–O	1.78	0.8	12.7	0.0017
			Mo–S	2.42	1.1	−5.0	0.0016
			Mo–Mo	3.16	1.2	−3.8	0.0110
CoS*x*–MoS*x*/NaY	2.1	2.1	Mo–S	2.41	5.0	−5.8	0.0020
			Mo–Mo	3.18	0.7	0.2	0.0079
			Mo–Co§	2.83	—	—	—
FeS*x*–MoS*x*/NaY	2.0	1.8	Mo–S	2.39	4.8	−5.5	0.0052
			Mo–Mo	3.17	0.9	−2.2	0.0056

*R: bond distance; CN: coordination number; E_0: inner potential; σ: Debye-Waller-like factor.
**Metal atoms/supercage.
†Sulfided at 673 K for 1.5 h.
††Sulfided at 673 K for 5 h.
§Bond distance was estimated using theoretical parameters.

Mo sulfide dimer species. On the other hand, the EXAFS results in Figure 3 for MoS_2/NaY show that Mo–O bondings remain after the sulfidation at 673 K, even for a prolonged sulfidation time (5 h).

The (average) compositions of the Mo sulfide species in MoS*x*/NaY and MoS_2/NaY were determined using XPS (S2*s*/Mo3*d* and S2*p*/Mo3*d* intensity ratios, S2$p_{3/2}$ = 162.0 ± 0.2 eV and S2*s* = 226.4 ± 0.2 eV) and XRF. They are summarized in Table 2. In agreement with the EXAFS results, it was found that the Mo sulfide species in MoS*x*/NaY were completely sulfided (S/Mo = 2), whereas those in MoS_2/NaY were only partially sulfided.

It was shown that at saturation two $Co(CO)_3NO$ molecules were accommodated per each supercage of NaY (2Co/SC, or 7.3 wt. % Co with respect to NaY). CoS*x*/NaY catalysts exhibited high HDS activities that are almost comparable to those of MoS*x*/NaY, as shown in Figure 1. However, Figure 2 shows that CoS*x*/NaY shows only a little HYD activity under the present reaction conditions. The HYD/HDS activity ratio was ca. 0.1 or from much lower than that for MoS*x*/NaY.

The k^3-weighted Fourier transforms of the Co K-edge EXAFS for CoS*x*/NaY and Co_9S_8 are compared in Figure 4. The Fourier transform for Co_9S_8 showed a convoluted peak at around 0.2 nm (uncorrected for the phase shifts), due to Co–S and Co–Co bondings, and a relatively weak peak at about 0.33 nm, due to Co–Co bondings in the third coordination sphere (Bouwens et al., 1991). On the other hand, with CoS*x*/NaY a peak attributable to Co–S bondings appeared separately at 0.17 nm with a weak shoulder peak at ca. 0.2 nm, obviously demonstrating a much weaker contribution from the Co–Co bondings in the second coordination sphere. No clear Fourier transform peak was observed at 0.33 nm. These findings clearly show that Co sulfide species prepared using $Co(CO)_3NO$ are highly dispersed in CoS*x*/NaY. As presented in Table 2, it is likely that the stoichiometry of CoS*x* species is slightly sulfur-rich compared to that of Co_9S_8 ($CoS_{0.89}$).

Table 2. Composition of Intrazeolite Metal Sulfides

Metal Sulfide	Loadings/SC Mo	Co/Fe	Composition	Technique
MoS*x*/NaY	2.0*		$MoS_{1.9-2.0}$	XPS
	1.9		$MoS_{2.1}$	XRF
MoS_2/NaY**	2.4		$MoS_{1.1}$	XPS
CoS*x*/NaY		2.1	$CoS_{1.0}$	XRF
FeS*x*/NaY		2.1	$FeS_{1.2}$	XRF
CoS*x*–MoS*x*/NaY	2.0*	2.0*	$Co_{2.0}Mo_{2.0}S_{5.8}$	XPS
	1.9	2.0	$Co_{2.0}Mo_{1.9}S_{5.7}$	XRF

*Chemical analysis using ICP and AAS; accuracy: ±0.1/SC.
**Prepared by an impregnation method.

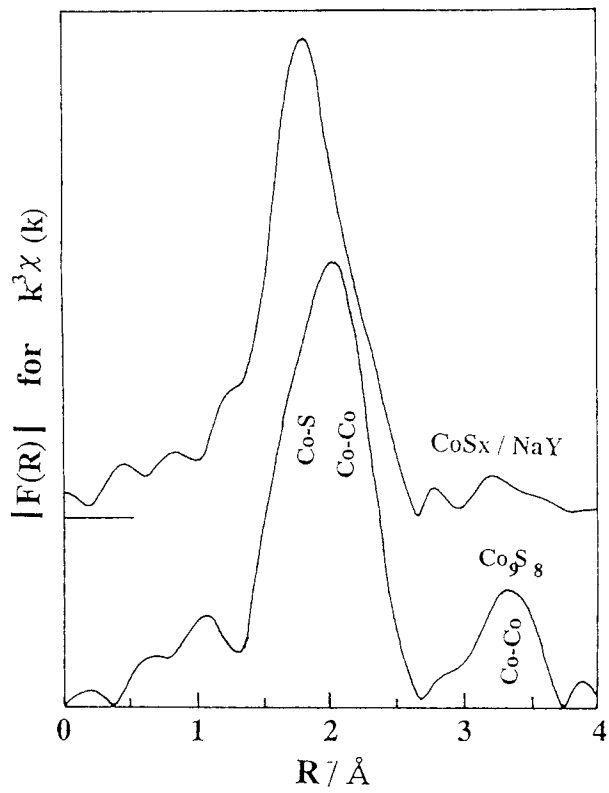

Figure 4. Fourier transforms of k^3-weighted EXAFS modulations (Δk = 4–15 Å^{-1}) of the Co *K*-edge for CoS*x*/NaY (2 Co/SC) and Co_9S_8.

FeSx/NaY prepared using $Fe(CO)_5$ as a precursor showed only a very low HDS activity at 673 K, as illustrated in Figure 1. On the basis of a Fe2p/Si2p XPS intensity ratio, it is estimated that this results partly from a large segregation of Fe sulfides over the external surface of the NaY zeolite during the sulfidation. XPS results showed that Fe was completely sulfided (Fe2$p_{3/2}$; 709.0 ± 0.2 eV).

Co–Mo binary sulfides encaged in NaY

The thiophene HDS activity of CoSx–MoSx/NaY, which possesses a constant amount of Mo (2.1Mo/SC or 12.5 wt. % Mo) is shown in Figure 5 as a function of Co content as expressed by the Co/Mo atomic ratio. The activity linearly increased as the Co content increased up to Co/Mo = ca. 1. The activity of CoSx–MoSx/NaY was higher than the sum of the activities of the corresponding MoSx/NaY and CoSx/NaY. Accordingly, it is concluded that the NaY-supported Co–Mo sulfide catalysts generate catalytic synergy between Co and Mo sulfides, with maximum HDS activity appearing at Co/Mo atomic ratio = ca. 1. On the other hand, FeSx–MoSx/NaY showed no catalytic synergies, as depicted in Figure 5.

The HDS activity in Figure 5 did not change when CoSx–MoSx/NaY was subjected to a prolonged sulfidation (20 h) at 673 K, indicating a high thermal stability of the catalytically active sulfide species. It was also found that, as long as the composition was identical, MoSx–CoSx/NaY, which was prepared by the introduction of $Mo(CO)_6$ to CoSx/NaY and the subsequent sulfidation at 673 K, exhibited the same HDS activities as CoSx–MoSx/NaY.

The activity of CoSx–MoSx/NaY for the HYD of butadiene was found to decrease only slightly as the Co content increased up to Co/Mo = 1, although the HYD activity of CoSx/NaY was very low compared to that of MoSx/NaY (Figure 2). Accordingly, the HYD/HDS activity ratio linearly decreased as the Co content and reached a ratio identical with that of Co sulfides at Co/Mo = 1. Besides, the butene selectivity in the butadiene HYD of CoSx–MoSx/NaY shifted upon the addition of Co from a *trans*-2-butene-rich composition, characteristic of Mo sulfides, to a 1-butene-rich one, characteristic of Co sulfides. The HYD selectivity of CoSx–MoSx/NaY was identical to that of CoSx/NaY at Co/Mo = 1.

Figure 6 illustrates the FTIR spectra of NO adsorbed on CoSx/NaY and CoSx–MoSx/NaY. Only the absorption positions are shown for MoSx/NaY for comparison. Nitric oxide molecules adsorb on Co or Mo sites, forming dinitrosyl complexes, and provide a pair of bands due to symmetric and asymmetric stretching vibrations (Okamoto et al., 1981; Topsøe and Topsøe, 1983). With CoSx/NaY, two peaks at 1,890 and 1,811 cm^{-1} were observed with a shoulder band at 1,865 cm^{-1}, suggesting the presence of two kinds of NO adsorption sites. In agreement with the observations for MoS_2/Al_2O_3, (Okamoto et al., 1981; Topsøe and Topsøe, 1983). MoSx/NaY showed two intense bands at 1,795 and 1,660 cm^{-1}. CoSx–MoSx/NaY exhibited doublet bands at 1,867 and 1,807 cm^{-1}, accompanying a shoulder band at ca. 1,880 cm^{-1}. These bands are apparently assigned on the basis of the band positions to the NO adsorbed on sulfided Co sites. It is noteworthy that with CoSx–MoSx/NaY (Co/Mo = 1), no IR peaks are observed that are due to the NO adsorbed on the Mo sulfide sites. It is concluded that, in spite of the simultaneous presence of the same amount of Mo sul-

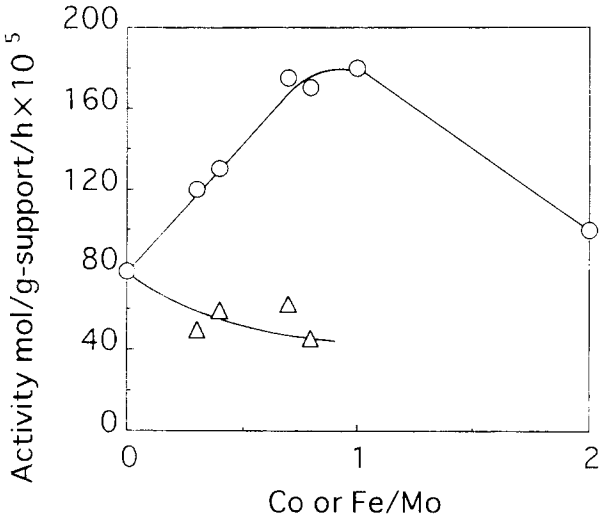

Figure 5. Catalytic activities of CoSx–MoSx/NaY (2.1 Mo/SC) and FeSx–MoSx/NaY (2.0 Mo/SC) as a function of Co or Fe content as expressed by Co(Fe)/Mo atomic ratio for HDS of thiophene.

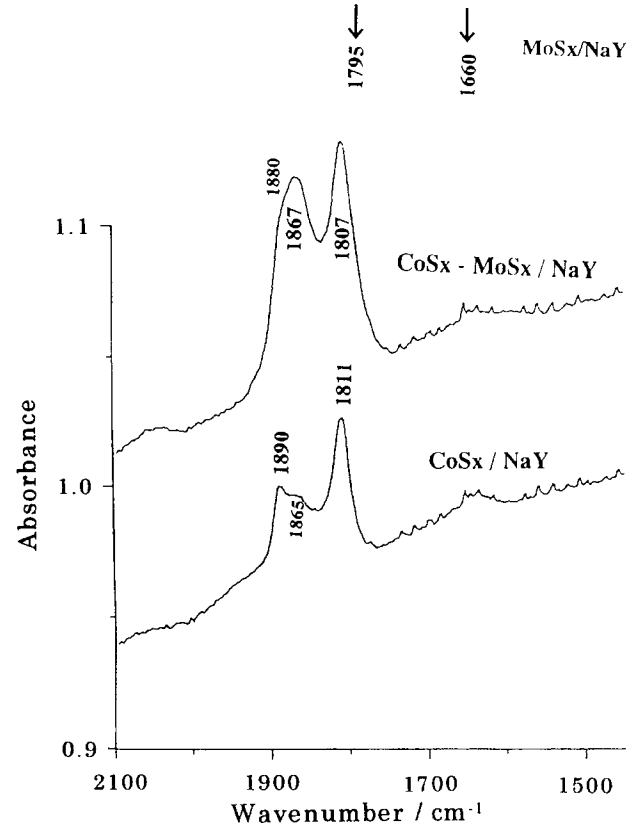

Figure 6. FTIR spectra of NO adsorption on CoSx/NaY (2.1 Co/SC) and CoSx–MoSx/NaY (2.1 Co+ 2.1 Mo/SC); peak positions for MoSx/NaY are shown for comparison.

fide species, coordinative unsaturation sites are formed only on Co sites.

Co–Mo binary sulfide catalysts were characterized by means of EXAFS, XPS, and XRF to reveal the formation of composite sulfides, electronic states, and composition. Figure 7 shows the k^3-weighted EXAFS functions, $k^3\chi(k)$, for MoSx/NaY (sulfided for 3 h for comparison), FeSx–MoSx/NaY, and CoSx-MoSx/NaY. The corresponding Fourier transforms are shown in Figure 8. MoSx/NaY

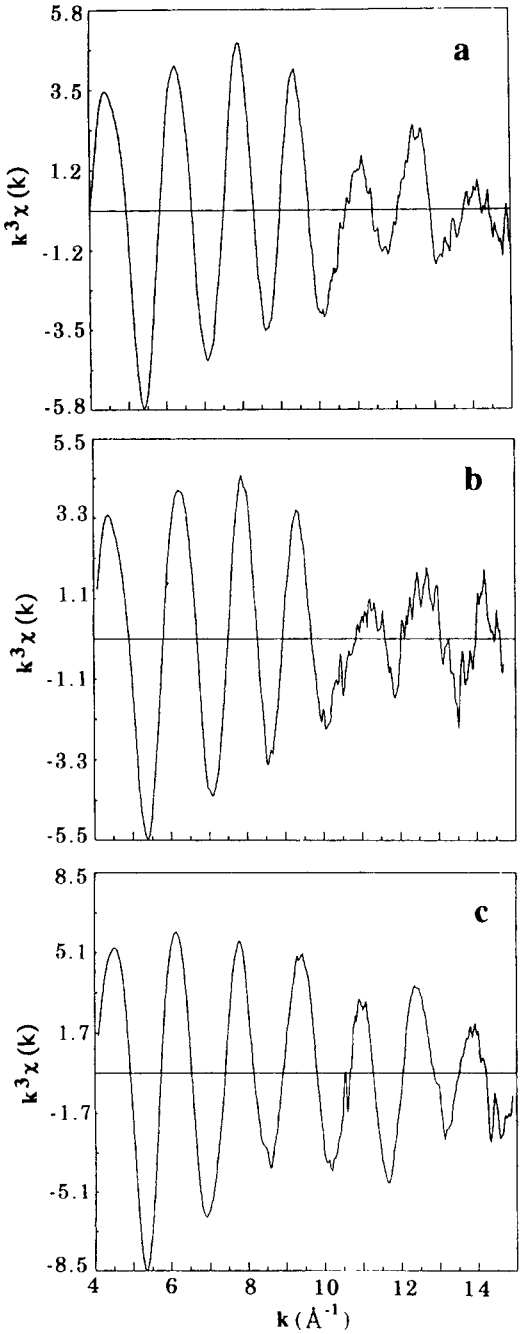

Figure 7. Background-subtracted k^3-weighted EXAFS functions, $k^3\ \chi(k)$, of the Mo K-edge for: (a) MoSx/NaY (2 Mo/SC, sulfided for 3 h); (b) FeSx–MoSx/NaY (2 Fe+2 Mo/SC); (c) CoSx–MoSx/NaY (2 Co+2 Mo/SC).

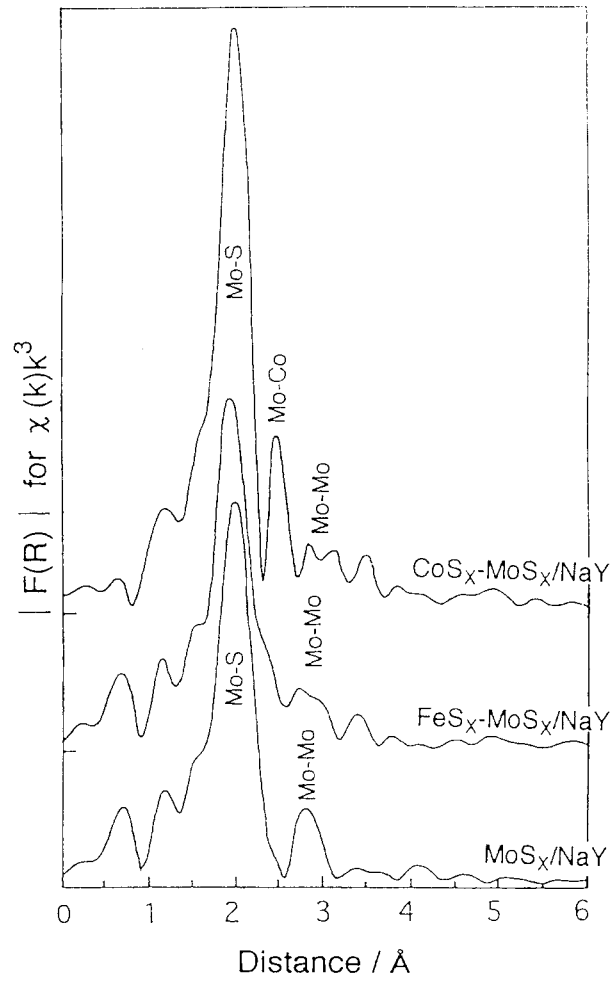

Figure 8. Fourier transforms of k^3-weighted EXAFS modulations (Δk = 4–15 Å^{-1}) of the Mo K-edge for MoSx/NaY (2 Mo/SC, sulfided for 3 h), FeSx–MoSx/NaY (2 Fe+2 Mo/SC), and CoSx–MoSx/NaY (2 Co+2 Mo/SC).

showed Mo–S and Mo–Mo bondings at 0.20 and 0.28 nm (uncorrected for phase shifts), respectively. With CoSx–MoSx/NaY, however, a new peak appeared at 0.24 nm in addition to the Mo–S and Mo–Mo bondings. These spectral features were reproducible in separate experiments. Since at present we have no experimental EXAFS parameters for Mo–Co bondings, we analyzed the peak using only the theoretical parameters calculated by Teo and Lee (1979). Using the theoretical EXAFS parameters, the analysis was found to provide correct atomic distances, for example, Mo–S (0.241 nm) and Mo–Mo (0.316 nm) bondings for MoS_2, although significantly smaller coordination numbers were obtained. It was found that the inverse Fourier transformed oscillation of the peak (ΔR = 0.232–0.268 nm) was reasonably curve-fitted (R factor; 10%) only when Mo–Co bondings were assumed. This may suggest that the peak at 0.24 nm is assigned to Mo–Co bondings. The structural parameters thus estimated are summarized in Table 1. The Mo–Co bond distance was estimated to be 0.283 ± 0.001 nm, which is consistent with those reported for supported Co–Mo binary sulfide catalysts (Bouwens et al., 1990, 1991, 1994). No Fourier

transform peak due to Mo–Fe bondings was observed for FeSx–MoSx/NaY, as shown in Figure 8.

The formation of the Co–Mo composite sulfides was examined by XPS for the NaY-supported Co–Mo binary sulfide catalysts. Figures 9 and 10 present the Mo3d and Co2p XPS spectra, respectively, for zeolite-supported Co–Mo binary sulfide catalyst systems. The Mo3d spectra for the catalysts prepared using $Mo(CO)_6$ showed an exclusive formation of MoS_2 (Mo3$d_{5/2}$; 228.9 eV). On the other hand, the convoluted spectra for MoS_2/NaY-based catalysts apparently indicated the simultaneous presence of the Mo^{5+} (230.7 eV) and Mo^{6+} (233.2 eV) species (Li and Hercules, 1984; Okamoto et al., 1989b; Okamoto et al., 1996c) together with MoS_2, demonstrating a partial sulfidation of the Mo species, which agrees with the EXAFS results in Figure 3. The spectral features of the Mo3d level were not altered by the addition of Co.

The Co2$p_{3/2}$ binding energy for CoSx-MoSx/NaY was 779.1 eV, which was higher by 0.6 eV than that for CoSx/NaY (778.5 eV), the binding energy of which is close to that for Co_9S_8 (778.4 eV) (Alstrup et al., 1982). In MoSx–CoSx/NaY, in which $Mo(CO)_6$ was introduced to CoSx/NaY, the Co2p XPS spectrum also showed the formation of Co sulfide species with a high Co2$p_{3/2}$ binding energy (779.3 eV). These high Co2p binding energies suggest the formation of specific Co sulfide species interacting with the preexisting or succeedingly admitted Mo sulfide species. On the other hand, CoSx/MoSx/NaY, prepared by using $Co_2(CO)_8$ instead of $Co(CO)_3NO$, showed a Co2$p_{3/2}$ binding energy at 778.4 eV, indicating that separate Co sulfide species are formed at least

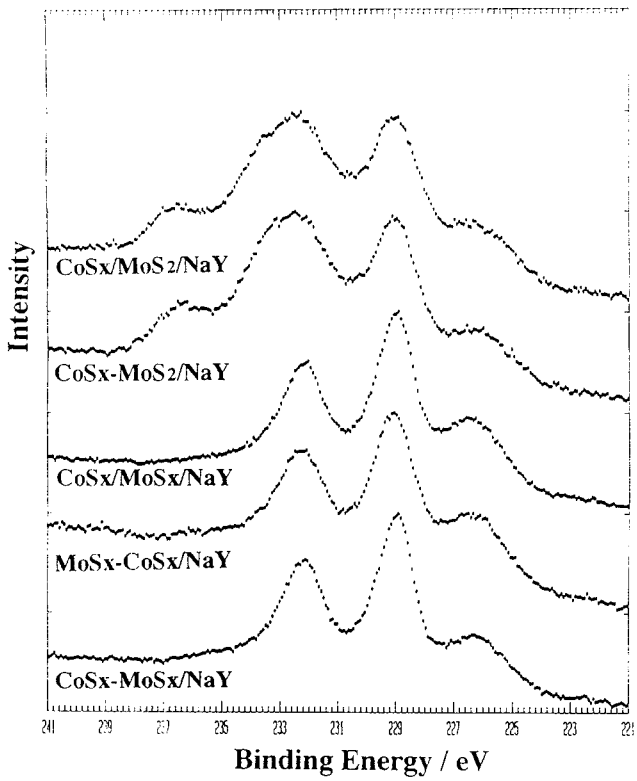

Figure 9. Mo3d XPS spectra for CoSx–MoSx/NaY, MoSx–CoSx/NaY, CoSx/MoSx/NaY, CoSx–MoS_2/NaY, and CoSx/MoS_2/NaY.

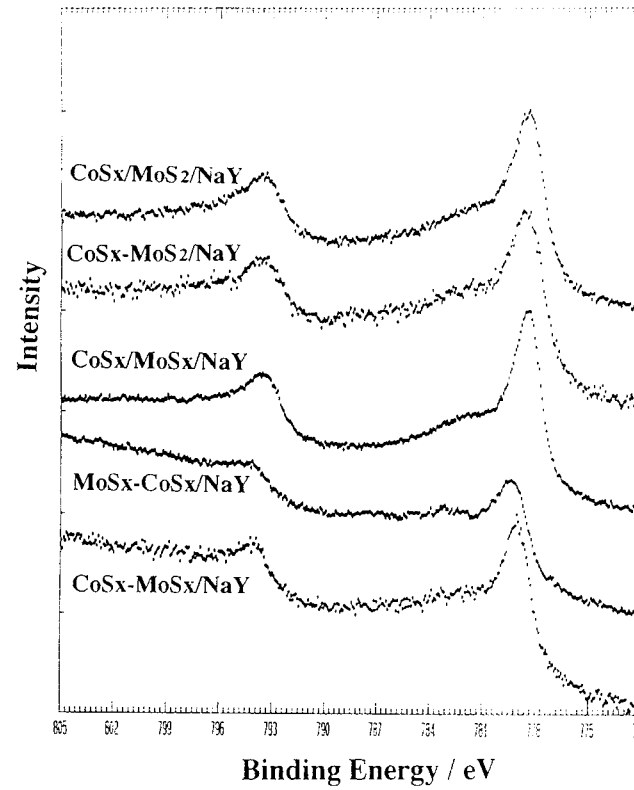

Figure 10. Co2p XPS spectra for CoSx–MoSx/NaY, MoSx–CoSx/NaY, CoSx/MoSx/NaY, CoSx–MoS_2/NaY, and CoSx/MoS_2/NaY.

on the outer surface of MoSx/NaY. Surface segregation of the Co sulfide species over the external surface of the zeolite in CoSx/MoSx/NaY (1.2 Co+2.1 Mo/SC) was indicated by a significantly higher Co2p/Si2p XPS intensity ratio (2.62), in spite of smaller Co content, than the ratio (1.21) for CoSx–MoSx/NaY (2.2 Co+2.1 Mo/SC). The Co2$p_{3/2}$ binding energies for the MoS_2/NaY-derived systems were consistent with that of Co_9S_8, suggesting that a majority of surface Co sulfide species is present as separate Co sulfides because of an incomplete sulfidation and poor dispersion (*vide infra*) of the Mo sulfide species in MoS_2/NaY.

The composition of catalytically active Co–Mo binary sulfide species was estimated by means of XPS and XRF. In the case of XPS, the area intensity ratios, S2p/Mo3d and S2s/Mo3d calibrated using MoS_2 as a reference, were used to calculate the S/Mo atomic ratio. The Co and Mo contents were obtained separately by chemical analysis. XRF measurements were made within a He atmosphere to prevent degradation of the sulfide samples by air oxidation. The composition thus obtained are summarized in Table 2. The XPS and XRF analyses of CoSx–MoSx/NaY provided an identical atomic ratio of 6/2/2 for S/Mo/Co.

Figure 11 depicts the catalytic activities of CoSx–MoSx/NaY and CoSx/MoSx/NaY for the HDS of thiophene in comparison with the corresponding simple sums of the activities of CoSx/NaY and MoSx/NaY, similarly prepared at the identical compositions. It was shown that a significant catalytic synergy was generated for CoSx–MoSx/NaY, while the activity of CoSx/MoSx/NaY was even lower than the total activity.

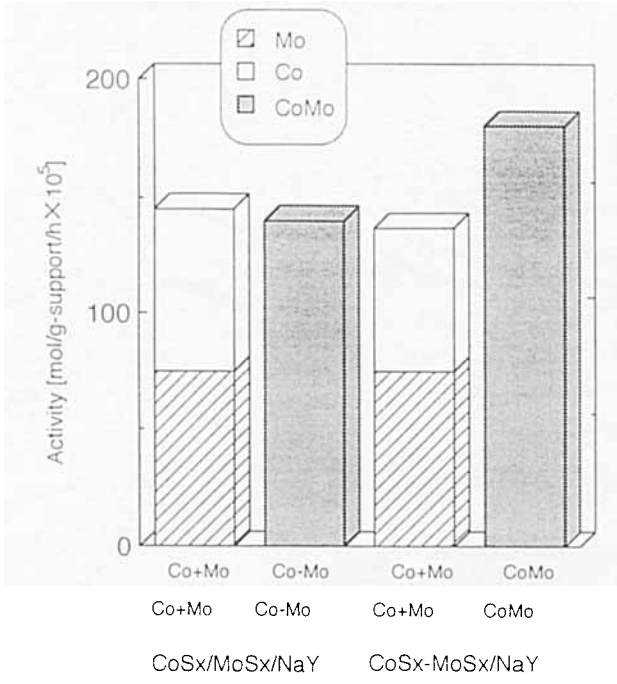

Figure 11. Activities of CoSx-MoSx/NaY (2 Co+2 Mo/SC) and CoSx/MoSx/NaY (1.2 Co+2 Mo/SC) for the HDS of thiophene; the corresponding sum activities of MoSx/NaY and CoSx/NaY (prepared using $Co(CO)_3NO$ or $Co_2(CO)_8$) are also shown for comparison.

Discussion

Intrazeolite Mo and Co sulfides

The EXAFS (Figure 3) and XPS (Figure 9) results on NaY-supported Mo sulfide catalysts indicate that the Mo sulfide species in MoSx/NaY are completely sulfided and highly dispersed. A complete sulfidation of the Mo species is also supported by the S/Mo atomic ratio in Table 2. In line with this, Vorbeck et al. (1994) showed the formation of stoichiometric Mo sulfide species by using $Mo(CO)_6$. Based on the combined results of high-resolution transmission electron microscopy (HRTEM), X-ray diffraction (XRD), relative HDS activities of substituted thiophenes, and pore volume measurements using benzene as an adsorbant (Okamoto et al., 1996c; Sakamoto et al., 1996), it has been demonstrated with MoSx/NaY that the pore structure of the host zeolite is not degraded by accommodating Mo sulfide clusters, and that finely dispersed Mo sulfide clusters are located in the zeolite cavities. It is therefore concluded that intrazeolite Mo sulfide clusters can be prepared using $Mo(CO)_6$ as a precursor.

On the other hand, current results using EXAFS, XPS, and sulfur analysis lead to the conclusion that Mo oxide species are only partially sulfided in MoS_2/NaY. It is estimated from the S/Mo ratio in Table 2 that the degree of sulfidation of MoS_2/NaY is about half under the present sulfidation conditions. In addition, the ratio of the coordination numbers, CN(Mo–Mo)/CN(Mo–S), is close to unity for crystalline MoS_2, suggesting poor dispersion of the Mo sulfide species in MoS_2/NaY. Partial sulfidation of conventional impregnation catalysts supported on zeolite has been reported by other workers (Leglise et al., 1988; Ezzamarty et al., 1989; Anderson et al., 1993; Vorbeck et al., 1994). This partial sulfidation of Mo is ascribed to the formation of tetrahedrally coordinated Mo oxide species during calcination (Cid et al., 1984; Okamoto et al., 1996a).

The higher HDS and HYD activities of MoSx/NaY are thought to result from a higher concentration of the active sites in MoSx/NaY than in MoS_2/NaY, due to the complete sulfidation of $Mo(CO)_6$ and a higher dispersion of the resultant Mo sulfide clusters. The same conclusions can be drawn from the fact that MoSx/NaY has a higher NO adsorption capacity than does MoS_2/NaY (Okamoto et al., 1989a; Laniecki and Zmierczak, 1991).

The EXAFS results in Figure 4 indicate that the Co sulfide species are highly dispersed. The high HDS activity of CoSx/NaY is attributed to the high dispersion of the Co sulfide species. Vissers et al. (1987) proposed that the high HDS activities of carbon-supported Co sulfide catalysts were due to the extremely high dispersion of the Co species. It is thought that the Co sulfide clusters in CoSx/NaY settle in the zeolite pores, since the HDS activities and Co2p XPS results for MoSx–CoSx/NaY were identical with those for CoSx–MoSx/NaY, in which Mo sulfide clusters, and thus the Co sulfide species interacting with the Mo sulfides are thought to be present in the pores. It is noteworthy that highly dispersed intrazeolite Co sulfide clusters are prepared using $Co(CO)_3NO$ adsorbed in NaY zeolite, even at a considerably high Co content (e.g., 2Co/SC or 7.3 wt. % Co).

Intrazeolite Co–Mo binary sulfides

The HDS activity of CoSx–MoSx/NaY (2.1 Mo/SC) increased linearly as the Co content increased, and reached the maximum at Co/Mo = ca. 1. The addition of Co into MoSx/NaY transformed the HYD/HDS activity ratio and HYD selectivity of MoSx/NaY into those of CoSx/NaY at the composition of the maximum HDS activity. These results can be understood neither in terms of a simple physical mixture of Mo and Co sulfide clusters, nor by a simple site blocking of the preexisting Mo sulfide species by successively added Co sulfides. The former possibility can be negated by the fact that Mo sulfide clusters show much higher HYD activity than Co sulfide clusters (Figure 2); the HYD selectivity would be Mo sulfidelike if the Mo and Co sulfide clusters independently catalyzed the HYD reaction. The latter mechanism is obviously excluded by the findings that, as long as the composition is identical, the same HDS activity is attained by MoSx–CoSx/NaY. Consequently, it is strongly suggested that intrazeolite binary sulfide clusters be synthesized using the metal carbonyl techniques.

The active sites of the Co–Mo binary sulfide clusters are thought to reside in the Co atoms rather than in the Mo atoms, since the catalytic properties of Co–Mo binary sulfide catalysts are very close to those of CoSx/NaY, except for the significantly enhanced activities, at the composition of the maximum HDS activity. This is clearly corroborated by the FTIR study of NO adsorption in Figure 6, which shows that with CoSx–MoSx/NaY (Co/Mo = 1) NO adsorbs exclusively on the Co sites. Equivalently, unsaturated sites are formed only on Co sites in spite of the simultaneous presence of the same amounts of Co and Mo sulfides. This is not explained assuming a simple mixture of highly dispersed Co and Mo

sulfide clusters in CoSx–MoSx/NaY. It is concluded that the HDS and HYD activities of the Co sulfide species are remarkably enhanced by combining with the Mo sulfide species.

The formation of Co–Mo binary composite sulfide clusters was examined using EXAFS and XPS techniques. An analysis of Mo K-edge EXAFS using the theoretical parameters suggests that the Fourier transform peak at 0.24 nm is because of Mo–CO bondings (0.283 nm). At present a lack of experimental parameters for the Mo–Co bondings restricts further analysis of the EXAFS data. Nevertheless, the reproducible EXAFS features in Figure 8 are thought to suggest the formation of Mo–S–Co chemical bonds, and thus of Co–Mo binary sulfide clusters. The Co *K*-edge EXAFS spectra for the Co–Mo binary sulfide systems are currently under study.

The XPS results provide direct and compelling evidence for the formation of Co–Mo binary sulfide clusters in CoSx–MoSx/NaY and MoSx–CoSx/NaY. It is evident from the Co2$p_{3/2}$ binding energies that specific Co sulfide species are formed in the Co–Mo sulfide systems prepared using $Mo(CO)_6$ and $Co(CO)_3NO$. Alstrup et al. (1982) reported a similar size of the Co2p chemical shift for the Co sulfide species interacting with the edge sites of MoS_2. It is therefore rational to assign the Co species to Co–Mo binary sulfide clusters. Taking into account the aforementioned catalytic properties, FTIR of NO adsorption, EXAFS results, and XPS binding energies, it is concluded that the Co–Mo binary sulfide clusters are fabricated exclusively in CoSx–MoSx/NaY and MoSx–CoSx/NaY at Co/Mo = 1. The binary sulfide clusters are thought to locate inside the zeolite cavities, since Mo sulfide clusters in MoSx/NaY are encaged in the pores, and the formation of Co–Mo binary sulfide clusters are not modified by the order in which Co and Mo are incorporating.

With CoSx/MoSx/NaY, the XPS results indicate a significant Co sulfide segregation on the surface, along with a separate sulfide formation. This is thought to result from a much slower diffusion of $Co_2(CO)_8$ into the zeolite pores because it has a larger molecular size than its mononuclear Co precursor, $Co(CO)_3NO$. In the case of MoS_2-derived catalysts, it is concluded that the Co sulfide species are present, thus forming a separate Co sulfide phase due to the incomplete sulfidation of the Mo species and the poor dispersion of the Mo sulfide species.

The composition of the Co–Mo binary sulfide clusters was estimated using XPS and XRF. The XPS and XRF techniques provided identical compositions, as shown in Table 2. It should be noted that the former technique provides a surface composition (< 5 nm) (Delgass et al., 1979), while the latter yields a bulk composition. Accordingly, it is concluded that the catalyst composition is homogeneous in depth.

As shown in Figure 5, the maximum HDS activity was attained at Co/Mo = 1 for CoSx–MoSx/NaY with 2 Mo/SC, and thus at 2 Co + 2 Mo/SC on average. Unfortunately, there is no direct evidence that Mo and Co atoms are homogeneously distributed across the zeolite cavities, forming a uniform Co–Mo composite sulfide species. However, there are some indications that a homogeneous Co–Mo binary sulfide compound is fabricated in each pore of the host zeolite: (1) the intrazeolite Mo sulfide species in MoSx/NaY (2 Mo/SC) consist of possibly two Mo atoms according to the EXAFS analysis in Table 1, which agrees with the average number of Mo atoms per SC; (2) the structure and dispersion of Mo (Co) sulfide clusters in MoSx (CoSx)/NaY seem to be homogeneous up to 2 Mo (Co)/SC, since the HDS and HYD activities increase linearly with the metal content; (3) the HDS activity of CoSx–MoSx/NaY increases in proportion to the Co content up to Co/Mo = 1; (4) the selectivity in the HYD of butadiene and the FTIR of NO adsorption indicate that there are no bare Mo sulfide sites exposed at Co/Mo = 1; and (5) the chemical composition of CoSx–MoSx/NaY is homogeneous in depth, as indicated by the identical XPS and XRF compositions. A clear Fourier transform peak due to Mo–Co bondings may indicate a definite local structure of Co–Mo composite sulfide clusters in CoSx–MoSx/NaY. It is therefore suggested that thermally stable and catalytically active Co_2Mo_2Sx clusters are formed in each supercage of the NaY host zeolite by means of the metal carbonyl techniques using $Mo(CO)_6$ and $Co(CO)_3NO$. The composition of the intrazeolite nanocomposite Co–Mo sulfides is shown to be $Co_2Mo_2S_6$ by using XPS and XRF. According to Halbert et al. (1985), a Mo sulfide dimer complex ($Mo_2S_4[(C_2H_5)_2NCS_2]_3$) reacts with $Co_2(CO)_8$ in a homogeneous system, forming a Co_2Mo_2 thiocubane complex. It is conjectured that analogous synthesis reactions take place in zeolite cavities between highly dispersed Mo sulfide clusters (possibly possessing dimer units according to the EXAFS in Table 2) and $Co(CO)_3NO$, or between highly dispersed Co sulfide clusters and $Mo(CO)_6$. Unfortunately, the structure of the composite clusters cannot be estimated at present because of a lack of experimental EXAFS parameters for Mo–Co bondings. A direct explanation of the composition and structure of the Co–Mo binary sulfide clusters must await further spectroscopic studies, including EXAFS, XRD, and UV–VIS and laser Raman spectroscopies.

FeSx–MoSx/NaY showed no catalytic synergies, as shown in Figure 5. The absence of Mo–Fe bondings in Figure 8 suggests that intrazeolite Fe–Mo binary sulfides are not formed under the present preparation conditions. The low thermal stability of the Fe–Mo binary sulfide phase (Karroua et al., 1992) may induce a separate phase formation, compared to that of the Co–Mo sulfide phase (Topsøe et al., 1996). The reduced HDS activity of FeSx–MoSx/NaY when Fe sulfides are added is thought to be caused, to a major extent, by the physical blockage of the active Mo sulfide sites by almost inactive Fe sulfide clusters.

In the case of intrazeolite nanostructure catalysts, some of the zeolite cavities are occupied by catalytically active species. The effects of reactant or product diffusions become more important and could modify the catalytic properties. With MoSx/NaY, about 25% of the pore volume was lost due to the accommodation of 2Mo/SC (Okamoto et al., 1996c). The activity ratio of tetramethylthiophene HDS/thiophene HDS over MoSx/NaY was found to be considerably smaller than that over MoS_2/Al_2O_3, in which diffusional effects are minimal because of the significantly larger pore size (19–20 nm) compared to that of NaY (0.74 nm) (Okamoto et al., 1996c). In addition, the HDS activity of MoSx/NaY, CoSx/NaY, and CoSx–Mo Sx/NaY increased in proportion to the number of intrazeolite metal sulfide clusters. Therefore, it is concluded that under the present reaction conditions intrazeolite metal sulfide clusters are catalytically active species and that no exclusive catalysis occurs at the pore openings because of the small molecular size of thiophene or butadiene.

Origin of catalytic synergies between Co and Mo sulfides

The results in Figure 11 show that catalytic synergy occurs in $CoSx$–$MoSx$/NaY, whereas there is no synergy in $CoSx$/$MoSx$/NaY. The difference is interpreted in terms of the catalyst structure and sulfide species. Based on the XPS results, it is suggested that with $CoSx$/$MoSx$/NaY, a considerable part of the Co is segregated over the external surface of $MoSx$/NaY, forming a separate Co sulfide phase. On the other hand, the EXAFS and XPS results for $CoSx$–$MoSx$/NaY clearly indicate the formation of the Co–Mo binary sulfide species encased in the zeolite. It is therefore most likely that the catalytic synergy between the Co and Mo sulfides is caused by the chemical bondings between them. The present results support the Co–Mo–S model proposed by Topsøe et al. (1984, 1986, 1996).

The XPS results of the increased Co2p binding energy on the formation of the Co–Mo binary sulfides suggest that an electron transfer from the Co to the Mo atoms activates the Co atoms in the clusters. A similar election transfer mechanism is proposed, based on the quantum chemical calculations by Harris and Chianelli (1986) for a Co-Mo binary sulfide cluster model. Riaz et al. (1994) recently showed that the desulfurization reactions of sulfur compounds in a liquid phase using a Co_2Mo_2 binary sulfide cluster, $Cp'_2Co_2Mo_2S_3(CO)_4$ (Cp': methylpentadiene), are initiated by a nucleophilic attack of sulfur compounds on the Co sites. The electron-deficient Co sulfide atoms in $Co_2Mo_2S_6$ are thought to facilitate the nucleophilic attack of thiophene in the initial stage of the HDS reaction, thereby increasing HDS activity. The roles of Mo sulfide in the Co–Mo binary sulfide catalysts are at least twofold; increase in the dispersion of Co sulfide species, and formation of electron-deficient Co species.

Conclusions

For the first time, it has been demonstrated by means of FTIR, EXAFS, XPS, and XRF that zeolite cavities are very suitable for the preparation and stabilization of highly dispersed and well-defined Mo, Co, and Co–Mo sulfide clusters. $Mo(CO)_6$ and $Co(CO)_3NO$ were found to be very useful as precursors for the preparation of the intrazeolite Co–Mo composite sulfide clusters. It is suggested that thermally stable nanocomposite $Co_2Mo_2S_6$ is formed in each cavity of a NaY zeolite. The Co–Mo binary sulfide clusters are catalytically active, showing synergies similar to those observed for conventional Co–Mo HDS catalysts. It has been shown that the Co sites of the clusters play a major role in the reactions. The intrazeolite nanocomposite approach is promising for precise investigations of catalysis on a molecular level, as well as for developing highly active and selective catalyst systems.

Acknowledgment

This work was carried out as a research project of The Japan Petroleum Institute, commissioned by the Petroleum Energy Center with a subsidy from the Ministry of International Trade and Industry. This work was also supported by a Grant-in-Aid for Scientific Research on Priority Area "Catalytic Chemistry of Unique Reaction Fields" (No. 08232251) from the Ministry of Education, Science, Sport and Culture. We are grateful to Prof. H. Kuroda and N. Kosugi for providing us with the EXAFS analysis program, and Prof. M. Nomura and the staff of the Photon Factory, National Laboratory for High Energy Physics, for assistance in measuring EXAFS spectra 90150 and 93G163). We express our thanks to Prof. M. Yamada (Tohoku University) and Messrs. M. Matsuo and K. Okuda (Rigaku Industrial Corp.) for the FTIR measurements and the XPS and XRF analyses of the catalysts, respectively. We express our gratitude to Prof. Shoichi Kimura (Oregon State University, Department of Chemical Engineering) for stimulating discussions.

Literature Cited

Alstrup, I., I. Chorkendorff, R. Candia, B. S. Clausen, and H. Topsøe, "A Combined X-Ray Photoelectron and Mössbauer Emission Spectroscopy Study of the State of Cobalt in Sulfided, Supported and Unsupported Co-Mo Catalysts," *J. Catal.*, **77**, 397 (1982).

Anderson, J. A., B. Pawelec, J. L. G. Fierro, P. L. Arias, F. Duque, and J. F. Cambra, "Mo-USY Zeolites for Hydrodesulfurization. II Surface Properties of Sulfided Catalysts and Activity for Thiophene Hydrodesulfurization," *Appl. Catal. A*, **99**, 55 (1993).

Bein, T., M. Tielen, and P. A. Jacobs, "Zeolite Supported Iron Oxide as Catalyst or Catalyst Precursor for Hydrocarbon Conversion Reactions," *Ber. Bunsenges. Phys. Chem.*, **90**, 395 (1986a).

Bein, T., G. Schmiester, and P. A. Jacobs, "Characterization of a New Iron-on-Zeolite Y Fischer-Tropsch Catalyst," *J. Phys. Chem.*, **90**, 4851 (1986b).

Bouwens, S. M. A. M., R. Prins, V. H. J. de Beer, and D. C. Koningsberger, "Structure of Molybdenum Sulfide Phase in Carbon-supported Mo and Co-Mo Sulfide Catalysts as Studied by Extended X-ray Absorption Fine Structure Spectroscopy," *J. Phys. Chem.*, **94**, 3711 (1990).

Bouwens, S. M. A. M., J. A. R. van Veen, D. C. Koningsberger, V. H. J. de Beer, and R. Prins, "Extended X-ray Absorption Fine Structure Determination of the Structure of Cobalt in Carbon-Supported Co and Co-Mo Sulfide Hydrodesulfurization Catalysts," *J. Phys. Chem.*, **95**, 123 (1991).

Bouwens, S. M. A. M., F. B. M. van Zon, M. P. van Dijik, A. M. van der Kraan, V. H. J. de Beer, J. A. R. van Veen, and D. C. Koningsberger, "On the Structural Differences between Alumina-supported CoMoS Type I and Alumina-, Silica-, and Carbon-supported CoMoS Type II Phases Studied by XAFS, MES, and XPS," *J. Catal.*, **146**, 375 (1994).

Breck, D. W., *Zeolite Molecular Sieves: Structure, Chemistry and Use*, Wiley, New York (1974).

Chianelli, R. R., M. Daage, and M. J. Ledoux, "Fundamental Studies of Transition-Metal Sulfide Catalytic Materials," *Adv. Catal.*, **40**, 177 (1994).

Cid, R., F. J. Llambias, J. L. Fierro, A. Lopez Agudo, and J. Villasenor, "Physicochemical Characterization of MoO_3-NaY Zeolite Catalysts," *J. Catal.*, **89**, 478 (1984).

Delgass, W. N., G. L. Haller, R. Kellerman, and L. H. Lunsford, *Spectroscopy in Heterogeneous Catalysis*, Chap. 8, Academic Press, New York (1979).

Delmon, B., "New Technical Challenges and Recent Advances in Hydrotreatment Catalysis. A Critical Updating Review," *Catal. Lett.*, **22**, 1 (1993).

Ezzamarty, A., E. Catherine, D. Cornet, J. F. Hemidy, A. Janin, J. C. Lavalley, and J. Leglise, "Characterization and Sulfidation of Stabilized HY Zeolites Containing Ni, Mo and NiMo Association," *Zeolite: Facts, Figures, Future*, P. A. Jacob and R. A. van Santen, eds., Elsevier, Amsterdam, p. 1025 (1989).

Fox, M. A., and T. L. Pettit, "Photoactivity of Zeolite-Supported Cadmium Sulfide: Hydrogen Evolution in the Presence of Sacrificial Donors," *Langmuir*, **5**, 1056 (1989).

Gates, B. C., J. R. Katzer, and G. C. A. Schuit, *Chemistry of Catalytic Processes*, McGraw-Hill, New York (1979).

Gates, B. C., "Supported Metal Clusters: Synthesis, Structure, and Catalysis," *Chem. Rev.*, **95**, 511 (1995).

Halbert, T. R., S. A. Cohen, and E. I. Stiefel, "Construction of Heterometallic 'Thiocubane' from $M_2S_2(\mu\text{-}S)_2$ Core Complexes: Synthesis of $Co_2M_2S_4(S_2CNEt_2)_2(CH_3CN)_2(CO)_2$ (M = Mo, W) and Structure of the $Co_2Mo_2(\mu_3\text{-}S)_4$ Cluster," *Organometallics*, **4**, 1689 (1985).

Harris, S., and R. R. Chianelli, "Catalysis by Transition Metal Sulfides: A Theoretical and Experimental Study of the Relation Between the Synergic Systems and the Binary Transition Metal Sulfides," *J. Catal.*, **98**, 17 (1986).

Herron, N., Y. Wang, M. M. Eddy, G. D. Stucky, D. E. Cox, K. Müller, and T. Bein, "Structure and Optical Properties of CdS Superclusters in Zeolite Host," *J. Amer. Chem. Soc.*, **111**, 530 (1989).
Ichikawa, M., "Metal Cluster Compounds as Molecular Precursors for Tailored Metal Catalysts," *Adv. Catal.*, **38**, 283 (1992).
Karroua, M., J. Ladriere, H. Matralis, P. Grange, and B. Delmon, "Characterization of Unsupported FeMoS Catalysts: Stability during Reaction and Effect of the Sulfiding Temperature," *J. Catal.*, **138**, 640 (1992).
Komatsu, T., S. Namba, and T. Yashima, "Preparation and Characterization of Mo/HNa-Y Zeolites," *J. Mol. Catal.*, **33**, 345 (1985).
Laniecki, M., and W. Zmierczak, "Thiophene Hydrodesulfurization and Water-Gas Shift Reaction over Molybdenum-Loaded Y-Zeolite Catalyst," *Zeolites*, **11**, 18 (1991).
Legliese, J., A. Janin, J. C. Lavalley, and D. Cornet, "Nickel and Molybdenum Sulfides Loaded into Zeolites: Activity for Catalytic Hydrogenation," *J. Catal.*, **114**, 388 (1988).
Li, C. P., and D. M. Hercules, "Surface Spectroscopic Study of Sulfided Molybdenum Alumina Catalysts," *J. Phys. Chem.*, **88**, 456 (1984).
Liu, X., and J. K. Thomas, "Formation and Photophysical Properties of CdS in Zeolites with Cages and Channels," *Langmuir*, **5**, 58 (1989).
Moller, K., T. Bein, S. Özkar, and G. A. Ozin, "Intrazeolite Phototopotaxy: EXAFS Analysis of Precursor $8\{W(CO)_6\}$-$Na_{56}Y$ and Photooxidation Products $16(WO_3)$-$Na_{56}Y$ and $28(WO_3)$-Na_{56} Y," *J. Phys. Chem.*, **95**, 5276 (1991).
Mortier, W. J., and R. A. Schoonheydt, "Surface and Solid State Chemistry of Zeolite," *Prog. Solid Chem.*, **16**, 1 (1985).
Okamoto, Y., Y. Katoh, Y. Mori, T. Imanaka, and S. Teranishi, "NO Adsorption Sites in Sulfided MoO_3/Al_2O_3 Catalysts," *J. Catal.*, **70**, 445 (1981).
Okamoto, Y., A. Maezawa, H. Kane, and T. Imanaka, "Thermal Stabilities and Catalytic Activities of Molybdenum Carbonyls Encaged in a Zeolite and Preparation of Molybdenum Sulfide Catalysts," *Proc. Int. Cong. Catal.*, Vol. 1, M. J. Phillips and M. Ternan, eds., The Chemical Institute of Canada, Ottawa, Ont., p. 11 (1988).
Okamoto, Y., A. Maezawa, H. Kane, and T. Imanaka, "Highly Dispersed Molybdenum Sulfide Catalysts Prepared from $Mo(CO)_6$ Encaged in a Zeolite," *J. Molec. Catal.*, **52**, 337 (1989a).
Okamoto, Y., A. Maezawa, and T. Imanaka, "Active Sites of Molybdenum Sulfide Catalysts Supported on Al_2O_3 and TiO_2 for Hydrodesulfurization and Hydrogenation," *J. Catal.*, **120**, 29 (1989b).
Okamoto, Y., T. Imanaka, K. Asakura, and Y. Iwasawa, "Structure and Electronic State of Molybdenum Subcarbonyl Species Encaged in Zeolite," *J. Phys. Chem.*, **95**, 3700 (1991).
Okamoto, Y., Y. Kobayashi, and T. Imanaka, "Structure of Molybdenum Oxide Clusters Prepared in Zeolite Cages," *Catal. Lett.*, **20**, 49 (1993).
Okamoto, Y., M. Odawara, H. Onimatsu, and T. Imanaka, "Preparation and Catalytic Properties of Highly Dispersed Molybdenum and Cobalt-Molybdenum Sulfide Catalysts Supported on Alumina," *Ind. Eng. Chem. Res.*, **34**, 3707 (1995a).
Okamoto, Y., "X-Ray Photoelectron Spectroscopic Characterization of Zeolites," *Crit. Rev. Surf. Chem.*, **5**, 249 (1995b).
Okamoto, Y., and H. Katsuyama, "Catalysis, and Characterization of Highly Dispersed Molybdenum Sulfide Catalysts Supported on a NaY Zeolite," *Ind. Eng. Chem. Res.*, **35**, 1834 (1996a).
Okamoto, Y., A. Kikuta, Y. Ohto, S. Nasu, and O. Terasaki, "Preparation, Characterization, and Catalysis of Intrazeolite Iron Oxide Clusters," *Progress in Zeolite and Microporous Materials*, H. Chon, S.-K. Ihm, and Y. S. Uh, eds., Elsevier, Amsterdam, p. 2051 (1996b).
Okamoto, Y., H. Katsuyama, K. Yoshida, K. Nakai, M. Matsuo, Y. Sakamoto, J. Yun, and O. Terasaki, "Dispersion and Location of Molybdenum Sulfides Supported on Zeolite for Hydrodesulfurization," *J. Chem. Soc., Faraday Trans.*, **92**, 4647 (1996c).
Ozin, G. A., and S. Özkar, "Intrazeolite Metal Carbonyl Phototopotaxy: From Tungsten (VI) Oxide Quantum Dots to a Zero-Dimensional Semiconductor Quantum Supralattice," *J. Phys. Chem.*, **94**, 7556 (1990).
Ozin, G. A., P. A. Prokopowicz, and S. Özkar, "Intrazeolite Nonstoichiometric Tungsten Oxides $n[WO_{3-x}]$-$Na_{56}Y$ ($0 < n < 32$, $0 < x < 1$)," *J. Amer. Chem. Soc.*, **114**, 8953 (1992a).
Ozin, G. A., S. Özkar, and R. A. Prokopowicz, "Smart Zeolites: New Forms of Tungsten and Molybdenum Oxides," *Acc. Chem. Res.*, **25**, 553 (1992b).
Prins, R., V. H. J. de Beer and G. A. Somorjai, "Structure and Function of the Catalyst and Promoter in Co-Mo Hydrodesulfurization Catalysts," *Catal. Rev.-Sci. Eng.*, **31**, 1 (1989).
Rabo, J. A., and G. J. Gajda, "Acid Function in Zeolites: Recent Progress," *Catal. Rev.-Sci. Eng.*, **31**, 385 (1989/1990).
Riaz, U., O. J. Curnow, and M. D. Curtis, "Desulfurization of Organic Sulfur Compounds Mediated by Molybdenum/Cobalt/Sulfur Cluster," *J. Amer. Chem. Soc.*, **116**, 4357 (1994).
Sachtler, M., and Z. Zhang, "Zeolite-supported Transition Metal Catalysts," *Adv. Catal.*, **39**, 129 (1993).
Sakamoto, Y., N. Togashi, O. Terasaki, T. Ohsuna, Y. Okamoto, and K. Hiraga, "MoS_2 Clusters in the Space of FAU Zeolite," *Mater. Sci. Eng. A*, **217/218**, 147 (1996).
Stucky, G. D., and J. E. MacDougall, "Quantum Confinement and Host/Guest Chemistry: Probing a New Dimension," *Science*, **247**, 669 (1990).
Schuit, G. C. A., and B. C. Gates, "Chemistry and Engineering of Catalytic Hydrodesulfurization," *AIChE J.*, **19**, 417 (1973).
Teo, B.-K., and P. A. Lee, "Ab Initio Calculations of Amplitude and Phase Functions for Extended X-ray Absorption Fine Structure Spectroscopy," *J. Amer. Chem. Soc.*, **101**, 2815 (1979).
Topsøe, N., and H. Topsøe, "Characterization of Structures and Active Sites in Sulfided Co-Mo/Al_2O_3 and Ni-Mo/Al_2O_3 Catalysts by NO Chemisorption," *J. Catal.*, **84**, 386 (1983).
Topsøe, H., and B. S. Clausen, "Importance of Co-Mo-S Type Structures in Hydrodesulfurization," *Catal. Rev.-Sci. Eng.*, **26**, 395 (1984).
Topsøe, H., B. S. Clausen, N. Topsøe, and E. Pederson, "Recent Basic Research in Hydrodesulfurization Catalysis," *Ind. Eng. Chem. Fundam.*, **25**, 25 (1986).
Topsøe, H., B. S. Clausen, and F. E. Massoth, "Hydrotreating Catalysis," *Catalysis-Science and Technology*, Vol. 11, J. R. Anderson and M. Boudard, eds., Springer-Verlag, Berlin (1996).
Vissers, J. P. R., V. H. J. de Beer, and R. Prins, "The Role of Co in Sulphidised Co-Mo Hydrodesulphurisation Catalysts Supported on Carbon and Alumina," *J. Chem. Soc., Faraday Trans. 1*, **83**, 2145 (1987).
Vorbeck, G., W. J. J. Welters, L. J. M. van de Ven, H. W. Zandbergen, J. W. de Haan, V. H. J. de Beer, and R. A. van Santen, "Zeolite Y Type Supported Nickel and Molybdenum Sulfides: Relations between Metal Sulfide Distribution and Catalytic Properties in Thiophene Hydrodesulfurization," *Zeolites and Related Microporous Materials: State of the Art*, J. Weitkamp, H. G. Karge, H. Pfeifer, and W. Hölderich, eds., Elsevier, Amsterdam, p. 1617 (1994).
Wang, Y., and N. Herron, "Optical Properties of CdS and PbS Clusters Encapsulated in Zeolites," *J. Phys. Chem.*, **91**, 257 (1987).
Wang, Y., and N. Herron, "Photoluminescence and Relaxation Dynamics of CdS Superclusters in Zeolites," *J. Phys. Chem.*, **92**, 4988 (1988).
Wark, M., G. Schulz-Ekloff, and N. I. Jaeger, "Particle Size and Photoabsorption of NaX Encapsulated CdS and PbS," *Catal. Today*, **8**, 467 (1991).
Yong, S. Y., and R. F. Howe, "Adsorption and Decomposition of $Mo(CO)_6$ in Zeolite NaY," *J. Chem. Soc., Faraday Trans. 1*, **82**, 269 (1986).

Manuscript received Oct. 28, 1996, and revision received Mar. 10, 1997.